論文 한국정밀공학회지 제12권 제9호 1995. 9
Journal of the Korean Society of Precision Engineering Vol.12. No.9. September. 1995.

3차원 절삭에서의 공구이탈시 발생하는 파단현상의 관찰및 해석

고 성 림,* David A. Dornfeld**

Observation and Analysis of Break Out at the Exit Stage in Oblique Cutting

Sung-Lim Ko,* David A. Dornfeld**

ABSTRACT

부품가공에 있어서 생산성향상을 위하여 버제거를 위한 고도의 기술이 더욱 중요하게되었다. 특히 CIM 체제에서는 버제거의 자동화를 위하여 가공중에 발생하는 버형성과 파단현상을 정량적으로 예측할 필요성이 더욱 커졌다. 이미 연구된 2차원절삭에서의 버형성 모델을 실제적인 3차원절삭에 적용하기 위하여 기존의 모델을 수정하는 작업이 이루어졌다. 3차원 절삭모델로는 절삭인선에 수직한 면에서의 칩과 공구의 상대운동에 의해서 결정된다고하는 Rubenstein의 가정이 사용되었다. 본연구에서 다루게되는 롤오버(roll-over) 버는 항상 공구진행방향으로 발생하기 때문에 3차원절삭에서의 버형성을 공구진행방향의 평면내에서의 2차원절삭의 집합으로 가정하였다. 공구의 기울림각(inclination angle)이 커질수록 버형성의 크기나 파단면의 크기가 감소하였다. 두종류의 파단이 버형성중에 관찰되었다. 하나는 가공물 끝면에 평행하게 파단면이 발생하였으며 다른 하나는 이에대하여 기울어진 파단이 일어났다. 가공물 끝면에 평행한 경우는 수정된 모델로부터 등가초기공구위치(equivalent initial tool distance)로부터 예측이 가능하며 기울어진 경우는 이결과와 공구의 기울림각으로부터 파단위치를 예측할 수있다.

Key Words : Burr(버), Oblique Cutting(3차원절삭), Burr Formation(버형성), Break Out(파단), Negative Shear Angle(음의 전단각), Tool Distance(공구위치), Inclination Angle(기울림각), Fracture Location(파단위치)

1. Introduction

A quantitative model of burr formation and fracture phenomenon in oblique cutting is suggested successively based on the model for orthogonal cutting. Considering that most machining processes like milling, turning and drilling involve oblique cutting, it is essential to modify the model for orthogonal cutting to describe the influence of obliquity on burr

* 건국대학교 기계설계학과
** University of California, Berkeley Department of Mechanical Engineering

formation. The previous works (1,2) are devided by two parts depending on the ductility of workpiece; fully ductile material without fracture during burr formation and the one with fracture. A quantitative burr formation model was previously suggested in orthogonal cutting when no fracture occurs, which is composed of three parts: initiation, development and final burr formation (1). A fracture criteron was introduced to predict the fracture phenomenon before the burr is fully formed during formation (2). The burr formation model in orthogonal cutting predicts the influence of the cutting conditions and material properties on burr formation. The cutting conditions used in orthogonal cutting are the undeformed chip thickness and tool rake angle. In oblique cutting the inclination angle, which is defined as the angle between cutting edge and the normal direction to the cutting direction, is added to the other conditions. Since burr formation can be considered as a special kind of chip formation, the model for chip formation in oblique cutting must be used appropriately and verified experimentally. Burr formations and fractures are observed in four kinds of workpieces; copper, alluminum alloys AL6061-T6, AL2024-T4 and cast aluminum AL390. Fully formed burrs are observed in copper. In AL6061-T6 and AL2024-T4, deformation and fractures, and in AL390, immediate fractures are observed during burr formation. According to the width of workpiece, two kinds of fractures are observed; uniform and inclined fracture in AL6061-T6 and AL2024-T4. The locations of fracture are predicted and compared with measurement values.

2. Burr Formation in Orthogonal Cutting

In this chapter, the burr formation and fracture model for orthogonal cutting suggested in previous works (1,2) are reviewed to help deriving the model for oblique cutting. A burr formation model in orthogonal machining was proposed previously when no fracture occurs (1). It is based on the assumption that the work done for chip formation is conserved for burr formation at transient point, A in Fig. 1, where chip formation stops and burr formation begins. The initiation of burr formation can be characterized by the initial negative shear angle, β_0, and the initial tool distance, ω, as shown in Fig. 1. After beginning burr formation at a position specified above, burr is developed according to the geometrical restriction that the plastic hinge point, B, is fixed during deformation. The interesting fact that the initial negative shear angle, β_0, is almost 20° regardless of workpiece material and cutting conditions is observed when exit angle is 90°. It was verified experimentally by other researchers. Hereafter 20° will be β_0 used for βo based on the experimental results. The initial tool distance can be obtained by equating the work for steady state chip formation to that for burr formation at transient point, A, (1).

$$\omega = \frac{\left[\dfrac{k_s}{\cos(\phi-\alpha)}\left\{\dfrac{t_0\cos\alpha}{\sin\phi}+sL\sin\phi\right\}\right]}{\left[\dfrac{k_0}{2}\cos^2\beta_0+\dfrac{\sigma_c}{4}\tan\beta_0\right]} \tag{1}$$

and

$$k_s=\frac{\overline{\sigma_0}}{\sqrt{3}}\left[\frac{\cos\alpha}{\sqrt{3}\sin\phi\cos(\phi-\alpha)}\right]^m \tag{2}$$

where k_s is the shear yield strength in the shear plane. s is the factor for the shear stress represented as, '0' and '1', when the chip is free and stuck fully on the tool rake

face respectively. t_o and L are the undeformed chip thickness and the tool/chip contact length in Fig. 1. $\overline{\sigma_0}$ and m are strain hardening coefficients from the relation between effective stress and strain, $\overline{\sigma} = \overline{\sigma_0}(\overline{\varepsilon^p})^m$. The initial tool distance, ω, can be also obtained using the cutting forces measured during chip formation as (1)

$$\omega = \frac{\dfrac{F_c}{\cos(\lambda-\alpha)\cos(\phi-\alpha)}[\cos\alpha\cos(\phi+\lambda-\alpha)+\sin\phi\sin\lambda]}{\left[\dfrac{k_0}{2}\cos^2\beta_0+\dfrac{\sigma_e}{4}\tan\beta_0\right]b} \quad (3)$$

where λ is friction angle obtained from $\tan(\lambda-\alpha)=F_V/F_C$. F_c and F_v are the measured cutting direction and normal direction forces, respectively.

As a result of comparison between the experiment and prediction by the model the assumption that the work for chip formation is converted to the work for initial burr formation at transient point is not always true due to the continuation of chip formation even after the initiation of burr formation. It turns out that the proportion of energy conversion for burr formation is dependent on the ductility which can be represented by the fracture strain in tension test (1). The proportion of energy conversion can be obtained from the ratio of initial tool distances from measurement and prediction in a specified material. The modified initial tool distance can be predicted as

$$\omega' = (ratio)\,\omega = \left(\frac{\omega_{meas}}{\omega_{pred}}\right)_{mat}\omega \quad (4)$$

where (*ratio*) for AL6061-T6 and AL2024-T4 were obtained as 0.51 and 0.54 experimentally (1).

Using the assumption that the plastic hinge point, B, is fixed during burr development and the burr formation continues without fracture until tool arrives at the end surface of workpiece, the final burr geometry is characterized as shown in Fig. 2 and can be obtained from the geometrical relation as follows (1).

$$h_f = (t_0+h_0)\sin\Psi_f = (t_0+\omega'\tan\beta_0)\sin(90^\circ-\beta_0) \quad (5)$$

where Ψ_f is the burr inclination angle, ω' is the modified initial tool distance, h_0 is the burr thickness and h_f is the final burr height.

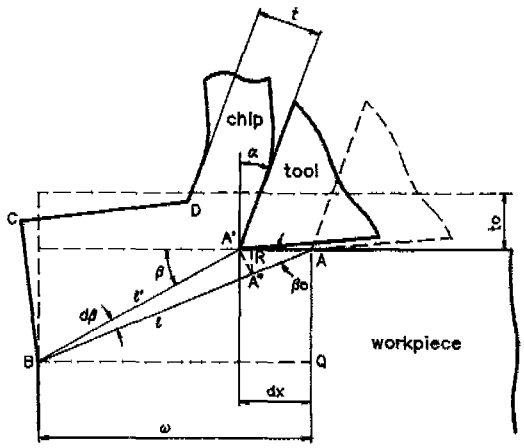

Fig. 1 Schematic Illustration of Initial Burr Formation

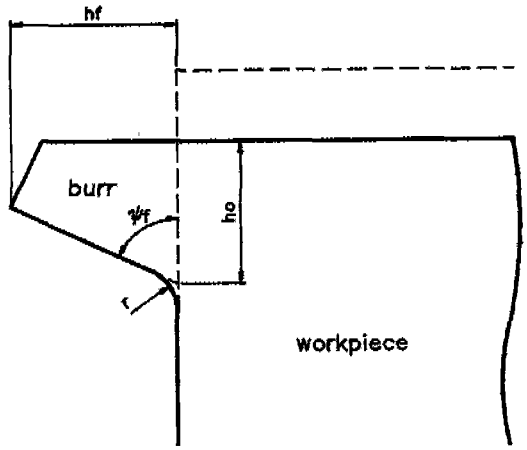

Fig. 2 Representation of Final Burr Formation Geometry

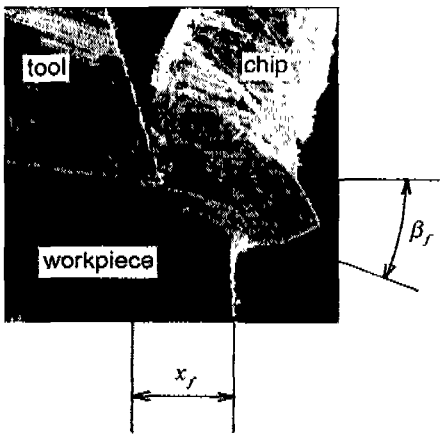

Fig. 3 Fracture during Burr Formation in machining AL6061-T6

In practice there is some reduction of the final burr height due to the compression around the plastic hinge point, B, during plastic bending deformation of the negative shear plane.

If fracture occurs during burr formation, the burr cannot be developed further. As the tool advances after the initiation of burr formation, the maximum strain, $\bar{\varepsilon}_{max}$, is obtained at the tool tip using the effective strain as follows(2)

$$\bar{\varepsilon}_{max} = \int_{\beta_0}^{\beta} \frac{\sqrt{2}}{3} \sqrt{\frac{6}{\beta^2} + \frac{3}{2\tan^4\beta}}\, d\beta \qquad (6)$$

where β_0 and β are the initial and current negative shear angle. As a fracture criterion, the fracture strain, ε_f, obtained in a tension test is used to predict the fracture. To check the validity of the fracture criterion, ε_f, obtained in tension test, ε_f in burr formation is obtained and compared (2). Fracture occurs when

$$\bar{\varepsilon}_{max} > \varepsilon_f \qquad (7)$$

The fracture during burr formation is characterized by the fracture negative shear angle, β_f, and the fracture location, x_f. In Fig. 3, fracture during burr formation is well illustrated in machining AL6061-T6, even though the tool is located at little bit advanced location after fracture occured. β_f can be obtained from equaions (6) and (7) and the fracture location, x_f, is determined from the geometrical relation (2),

$$\omega' \tan\beta_0 = x_f \tan\beta_f \qquad (8)$$

where ω' is modified initial tool distance.

3. Burr Formation in Oblique Cutting

Since the burr formation model in equations (1) and (3) is closely related to the chip formation, it is necessary, in order to be able to modify the burr formation model for orthogonal cutting to that for oblique cutting, to understand the chip formation in oblique cutting. Usui et. al (3) analyzed the oblique cutting process as a piling up of orthogonal cutting in the plane containing cutting velocity V and chip velocity V_c along the cutting edge. Rubenstein's analysis is based on the realization that the chip removal occurs as a result of the "normal" tool/workpiece relative movement while the "lateral" movement causes the chip to flow at an angle η_c to the line of greatest slope of the rake face (4). Using Rubenstein's oblique cutting model, the shear plane angle, ϕ_n, in oblique cutting, Fig. 4, can be determined from the shear plane angle in orthogonal cutting, ϕ_O.

$$\cot\phi_n = \cot\phi_0 \cos i - \tan\alpha_n(1-\cos i) \qquad (9)$$

In the model development for burr formation in oblique cutting, Rubenstein's chip formation model will be used based on his continuous work (5) which verifies his model. It is much easier to implement than Usui's model using effective angles.

When modifying the burr formation model for orthogonal cutting into the model for

oblique cutting, it is helpful to realize that the rollover burr is formed in the cutting direction. Therefore only the cutting force components in the cutting direction plane, F_c and F_t, will be used in the analysis of the rollover burr. Burr formation in oblique cutting can be assumed as the accumulation of burr formation of orthogonal cutting in the cutting direction because rollover burrs are formed only in cutting direction. From Rubenstein's chip formation model in oblique cutting (4), the actual chip formation occurs in the cutting plane normal to cutting edge, plane *POQ* in Fig. 4. Thus, the relation between α_n and ϕ_n is assumed to be same as in orthogonal cutting. The chip formation in the normal cutting plane is characterized by undeformed chip thickness, t_0, normal rake angle, α_n, shear plane angle, ϕ_n, and tool/chip contact length, L. The equivalent orthogonal cutting is constrained to have same chip thickness and normal component of chip velocity by using the reduced undeformed chip thickness, $t_0 \cos i$, and the same cutting speed. The chip formation in segmented orthogonal cutting in the cutting direction plane, plane

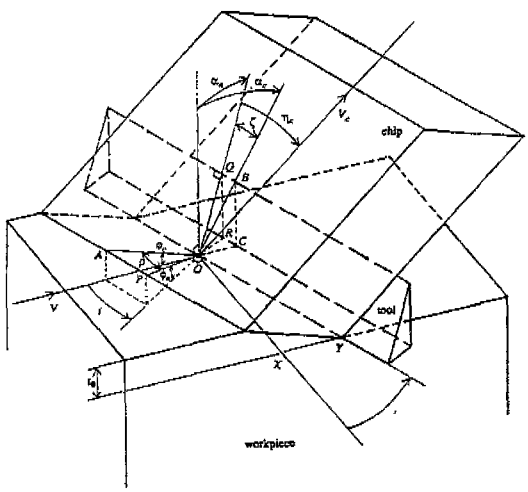

Fig. 4 Schematic Illustration of Oblique Cutting

AOB in Fig. 4, can be represented by the undeformed chip thickness, t_0, tool rake angle, α_c, shear palne angle, ϕ_c, and tool/chip contact length, L_c. The shear plane angle and the rake angle in the cutting direction plane can be determined geometrically in Fig. 4 as follows.

$$\phi_c = \tan^{-1}(\tan\phi_n \cos i) \tag{10}$$

$$\alpha_c = \tan^{-1}\left(\frac{\tan\alpha_n}{\cos i}\right)$$

where the shear plane angle in the normal plane is derived in equation (9). The tool/chip contact length, L_c, is obtained from Fig. 4 and Rubenstein's result (6) as

$$L_c = \frac{1}{\cos\xi}\left[\frac{rt_0 \cos i \sin(\phi_n + \lambda_n - \alpha_n)}{\sin\phi_n \cos\lambda_n}\right] \tag{11}$$

where

$$\xi = \tan^{-1}(\sin\alpha_n \tan i) \tag{12}$$

and γ can be determined experimentally (6).

The initial tool distance, ω, can be obtained by substituting equations (10) and (11) into equation (1).

$$\omega = \frac{\dfrac{k_s}{\cos(\phi_c - \alpha_c)}\left[\dfrac{t_0 \cos\alpha_c}{\sin\phi_c} + sL_c \sin\phi_c\right]}{\left[\dfrac{k_0}{2}\cos^2\beta_0 + \dfrac{\sigma_e}{4}\tan\beta_0\right]} \tag{13}$$

where

$$k_c = \frac{\overline{\sigma_0}}{\sqrt{3}}\left[\frac{\cos\alpha_n}{\sqrt{3}\sin\phi_n \cos(\phi_n - \alpha_n)}\right]^m \tag{14}$$

When modifying the force implemented burr formation model in orthogonal cutting, equation (3), the geometrical quantity in equation (10) can also be used. But the cutting forces measured during oblique cutting cannot be used directly. The work for chip formation is described as

$$\Delta W_{chip} = F_s ds + F_f df$$

where F_s and F_f are the forces in the shear plane and on the tool rake face, respectively. Now the work for chip formation which will be used for burr formation in oblique cutting can be represented as

$$\Delta W_{chip} = (F_s \cos\kappa) ds + (F_f \cos\chi) df \qquad (15)$$

where cos κ and cos $\varkappa$ represent the cosines of the shear plane POY and the friction plane QOY to the plane AOX and BOX in Fig. 4 respectively.

$$\cos\kappa = \frac{\cos i}{\cos\xi}$$

$$\cos\chi = \frac{\cos i}{\cos\rho} = \frac{\cos i}{\frac{\sin\phi_c}{\sin\phi_n}}$$

Using the geometrical relation for cos κ and cos $\varkappa$, the initial tool distance for burr formation in oblique cutting becomes

$$\omega = \frac{\frac{F_c}{\cos(\lambda_c - \alpha_c)\cos(\phi_c - \alpha_c)}[\cos\alpha_c \cos(\phi_c + \lambda_c - \alpha_c)\cos\kappa + \sin\phi_c \sin\lambda_c \cos\chi]}{\left[\frac{k_0}{2}\cos^2\beta_0 + \frac{\sigma_e}{4}\tan\beta_0\right] b} \qquad (16)$$

Considering that as the inclination angle increases the cutting direction force, F_c, does not change much and the angles between the shear plane and the plane AOX and between the tool rake face and the plane BOX increase, the initial tool distance predicted by equation (16) will decrease. Using the predicted initial tool distance in equations (13) and (16), the modified initial dool distance can be obtained from equation (4). Here it is assumed that the energy conversion ratio for burr formation in orthogonal cutting can also be applied for oblique cutting. Using the modified initial tool distance, ω', development of burr formation or fracture prediction can be analyzed in the same process as in the orthogonal cutting.

4. Observation and Analysis of Fracture in Oblique Cutting

Copper, aluminum alloys AL6061-T6 and AL2024-T4 and cast aluminum AL390 were cut to check the validity of the model for chip formation and burr formation in oblique cutting. The copper is annealed and considered to be a very ductile material. Cast aluminum AL390 is considered very brittle. Aluminun alloys AL6061-T6 and AL2024-T4 have intermediate material properties. These mechanical material properties are listed in Table 1.

4.1 Observation of Burr Formation and Fracture in Oblique Cutting

The experimental set-up on the modified milling machine which enables orthogonal and oblique cutting by changing tool inclination angle is used to observe the burr formation in several materials. Three undeformed chip thicknesses, 0.1, 0.15 and 0.2mm. and two cutting speeds, 66.8 and 508 mm/min are used. For oblique cutting, three inclination angles, 0°, 20° and 40°, are used. The tool rake angle is 10° and the

Table 1 Material Properties of Workpieces

* obtained from reference (7,8)
** obtained from reference (9) and the fracture strain is obtained from reference (10)

Property / Material	Tensile Strength σ_t(ksi)	Yield Strength σ_e(ksi)	Work Hardening Property $\overline{\sigma_0}$	Work Hardening Property m	Fracture Strain ε_f
Cu*	32 (220Mpa)	10 (69Mpa)	46.4 (496Mpa)	0.54	2.30
AL6061-T6**	45(310)	40(275)	60(414)	0.05	0.50
AL2024-T4*	68(469)	47(324)	100(689)	0.15	0.13
AL390*	41(283)	35(242)	41(283)	≒0.0	≒0.0

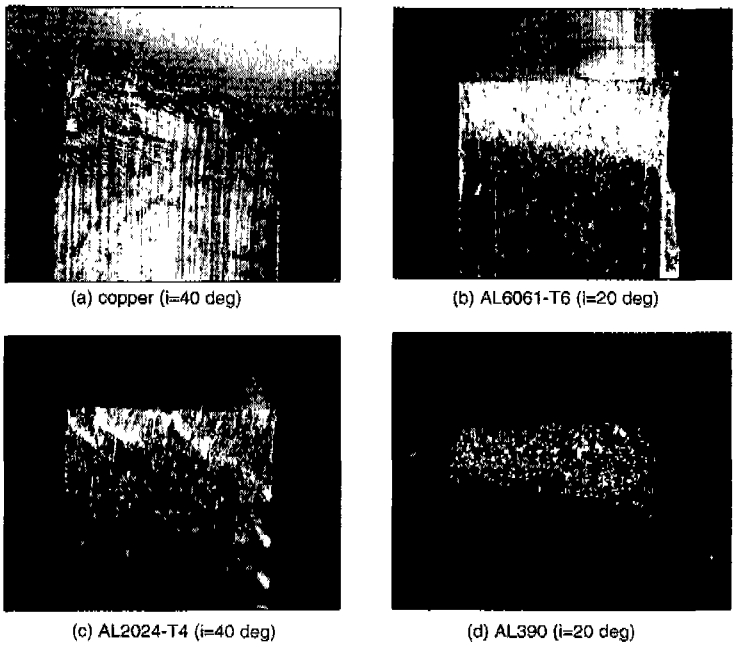

Fig. 5 Observation of Burr Formation and Fracture in Oblique Cutting

width of workpiece is 3.17mm.

Photographs in Fig. 5 show some typical results in this experiment. In Fig. 5(a) burr is formed without fracture in copper. Even though the burr is expected to be formed uniformly, the variation of burr height in copper is attributed to the severe chip distorsion. Due to this severe chip distorsion, it is proved that it is not appropriate to apply the Rubenstein's model for copper. The prediction of burr height by the model in equation (13) is dependent on the cutting conditions, like undeformed chip thickness and rake angle, and on the material properties, like strain hardening coefficients ($\overline{\sigma_0}$, m) and coefficient of tool/chip contact length(γ). When t_0 = 0.2mm, α = 10°, $ratio$ = 0.15, s = 0.5, 0.8 and 1.0 and r is assumed to be 2.0, the predicted burr height, $(h_f)_{pred}$, in copper is plotted in Fig. 6. It is seen that the burr height decreases as the inclination angle, i, increases. In Fig. 5(b)-(d) fractures are observed. Whereas Fig. 5(b) shows inclined fracture in AL6061-T6 with 20° inclination angle, in Fig. 5(c) the combination of uniform and inclined fracture is observed in AL2024-T4 with 40° inclination angle. In AL390 different kind of fracture occurs due to the brittle property. The configuration of fracture is dependent on the inclination angles and width of workpiece. It is noted that whereas the size of the frac-

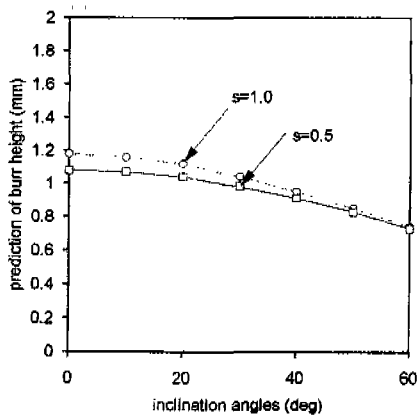

Fig. 6 Variation of Burr Height in copper

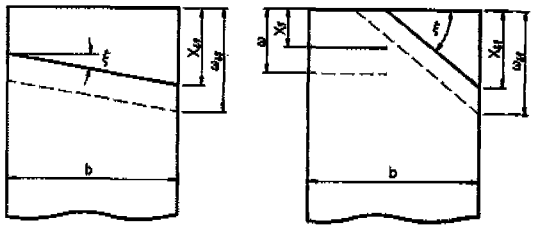

(a) $i=20°$ (b) $i=40°$

Fig. 7 Configuration of Fracture Surface in Oblique Cutting

ture in orthogonal cutting is constant along the cutting edge, that is not the case in oblique cutting. This may be due to the fact that there is a transient phenomenon when the tool approaches the last corner of the workpiece as shown in Fig. 7. When the uniform fracture occurs as in orthogonal cutting, the location of fracture, x_f in equation (8), can be determined from equations (8), (13) and (16). However the uniform fracture in oblique cutting cannot occur when the tool approaches the last corner of workpiece as shown in Fig. 7 due to the fracture along cutting edge. The location of inclined fracture, x_{if}, around the last corner is dependent on the width of workpiece and tool inclination angle.

4.2 Analysis of Inclined Fracture in Oblique Cutting

As the tool advances to the last corner in Fig. 7, two kinds of fractures occur at different distance, x_{if}, in AL6061-T6, AL2024-T4 and AL390 as shown in Fig. 5(b)-(d). In the workpiece wide enough at a given inclinatin angle, both the uniform and inclined fractures exist as in Fig. 5(c) and Fig. 7(b) when i = 400. The uniform fracture has the fracture surface parallel to the end of workpiece whereas the inclined fracture occures along the cutting edge.

When i = 20° in Fig. 5(b) and (d), because the width of the workpiece is not sufficient no uniform fracture exists and only the inclined fracture occurs along the cutting edge. The inclined fracture can be specified by x_{if} and ξ in Fig. 7(a). The initiation of deformation is assumed to begin parallel to the fracture line in Fig. 7(a) according to the relation, $\omega' \tan \beta_O = x_f \tan \beta_f$ in equation (8). Since the fracture location varies along the cutting edge of the tool in Fig. 7 the initial tool distance can represented in both cases as

$$\omega(y) = \omega_{if} - \tan \xi \, y \tag{17}$$

where ω_{if} is the initial tool location for inclined fracture and y is the axis in the thickness direction. The work for initiation of burr formation in orthogonal cutting can be obtained as (1)

$$\Delta W_{burr} = \left[\frac{k_0}{2}\cos^2\beta_0 + \frac{\sigma_c}{4}\tan\beta_0\right] \omega \, b \, dx$$

where b is thickness of workpiece. It can be modified for the case that only inclined fracture, as in Fig. 7(a), exists as followes

$$\Delta W_{burr} = \left[\frac{k_0}{2}\cos^2\beta_0 + \frac{\sigma_c}{4}\tan\beta_0\right] \left[\int_0^b \omega(y)dy\right] dx$$

or,

$$\Delta W_{burr} = \left[\frac{k_0}{2}\cos^2\beta_0 + \frac{\sigma_c}{4}\tan\beta_0\right] \omega'_{eq} b \, dx \tag{18}$$

where ω'_{eq} is modified from eqivalent initial tool distance, ω_{eq}. The equivalent initial tool distance, ω_{eq}, can be considered as the initial tool distance predicted by equations (13) and (16) for uniform fracture in oblique cutting. To predict the fracture location, $(x_f)_{pred}$, using the predicted initial tool distance, $\omega = \omega_{eq}$, the ratio of energy conversion for burr formation must be considered as in equation (4) to obtain the inclined fracture location, ω_{if}.

$$\omega'_{eq} = \omega_{eq}\ ratio = \omega_{if} - \frac{1}{2}\tan\xi\, b \qquad (19)$$

Using ω_{if} obtained here, x_{if} can be determined from $\omega_{if}\tan\beta_O = x_{if}\tan\beta_f$.

When $i = 40^\circ$, the uniform fracture location, x_f, and the inclined fracture location, x_{if}, are well distinguished in Fig. 5(c) and in Fig. 7(b). x_f can be obtained from equations (4), (8), (13) and (16). The final fracture when i = 40° is specified by the inclined fracture location, x_{if}, and the fracture angle, ξ, which is close to the inclination angle in Fig. 7(b). When the tool arrives at the initial position for transient fracture in Fig. 7(b) the work for initial burr formation is similarly obtained as in the case for i = 20°.

$$\Delta W_{burr} = \left[\frac{k_0}{2}\cos^2\beta_0 + \frac{\sigma_e}{4}\tan\beta_0\right]\left[\int_0^{\beta}\omega(y)dy\right]dx$$

or,

$$\Delta W_{burr} = \left[\frac{k_0}{2}\cos^2\beta_0 + \frac{\sigma_e}{4}\tan\beta_0\right]\omega'_{eq}a\,dx \qquad (20)$$

where a is the width of workpiece at the moment of initial transient fracture. Since ω_{eq} is the initial tool distance predicted from equation (13) and (16), it must be modified to be used for obtaining the actual initial tool distance, ω_{if}, using the relation, ω_{if} = a tan ξ,

$$\omega'_{eq} = \omega_{eq}\ ratio = \omega_{if} - \frac{1}{2}\tan\xi\, a = \frac{1}{2}\tan\xi\, a \qquad (21)$$

where $(ratio)_{A16061\text{-}T6} = 0.51$ and $(ratio)_{A12024\text{-}T4} = 0.54$. In the same way as in i = 200, the initial fracture location for the inclined fracture, ω_{if} or a, can be obtained using ω_{eq} from equation (13) and (16). x_{if} can be obtained from ω_{if} using $\omega_{if}\tan\beta_O = x_{if}\tan\beta_f$. From two cases of inclined fracture in equations (19) and (21) the critical

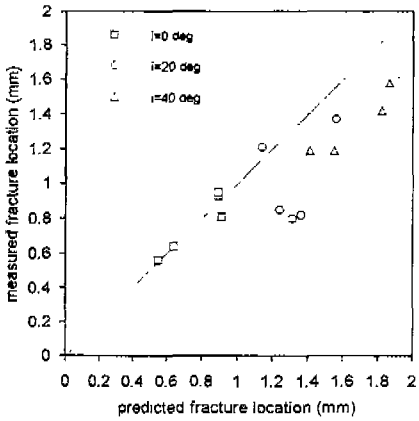

Fig. 8 Comparison of Inclined Fracture Location in AL6061-T6

width of workpiece for the existence of uniform fracture is

$$b > \frac{2\omega'_{eq}}{\tan\xi} \qquad (22)$$

where ξ is assumed to be same as the inclination angle i.

The cutting forces in cutting direction and feed direction, F_c and F_v, shear angle, ϕ_n, and the fracture geometries, x_f, x_{if}, ξ, and β_f, are measured according to the inclination angle and workpiece material. The inclined fracture locations, x_f, are predicted as analyzed before. $ratio$, $\omega_{meas}/\omega_{pred}$, which is determined for $i = 0^\circ$ in each material is used for $i = 20^\circ$ and 40°. In both materials, AL6061-T6 and AL2024-T4, the slope of inclined fracture, ξ, ranges from 8° to 17° when $i = 20^\circ$ and it ranges from 40° to 45° when $i = 40^\circ$. It is observed that larger the inclination angle becomes the inclined facture occurs closer to the inclination angle. Based on this observation the slope of fracture, ξ, can be assumed to be same as the inclination angle, i. The predicted and measured inclined fracture locations, x_{if} when $i = 0^\circ$, 20° and $i = 40^\circ$ are compared in Fig. 8 for AL6061-T6 and Fig. 9 for AL2024-T4. Each data are

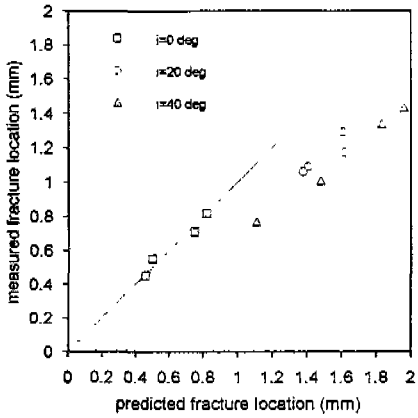

Fig. 9 Comparison of Inclined Fracture Location in AL2024-T4

obtained from equations (16), (19) and (21) using the force measured during cutting. Therefore the conditions in Fig. 8 and 9 keep different undeformed chip thickness but same tool rake angle 10° and cutting speed 508 mm/min. It turns out that the accuracy of predictions are related to that of angle of inclined fracture, ξ. In the case of orthogonal cutting, when $i=0°$, the predictions are successfully carried out as shown in previous work (2). However when $i=20°$, only inclined fractures exist and the prediction of fracture locations, x_{if}, is poor due to the poor prediction for the angle of inclined fracture. When $i=40°$, both the uniform and inclined fractures exist. As shown in Fig. 5(c), some fructuations are observed even in uniform fracture and this makes it difficult to measure an exact fracture location. The predictions for the angle of inclined fracture is more accurate than when $i=20°$. The predicted fracture locations are mostly larger than measured values.

In the case of cast aluminum AL390, the configuration of fracture is quite different from that of AL6061-T6 and AL2024-T4 as shown in Fig. 5(d). The measured fracture negative shear angle, β_f, ranges 35°-45° regardless of the inclination angles. It seems that fracture occures along the plane of maximum infinitesimal normal strain in brittle material without plastic deformation. More research for the fracture in brittle material must be continued.

5. Conclusion

Using the burr formation and fracture model for orthogonal cutting suggested in previous work, a modified burr formation model including the fracture phenomenon in oblique cutting is proposed. It is based on the fact that the rollover burr is formed in the cutting direction and the oblique cutting is an accumulation of segmented orthogonal cutting.

As a chip formation model in oblique cutting, Rubenstein's model that the chip formation occures in the plane normal to cutting edge is used. In the case of ductile material like copper, the application of Rubenstein's model for oblique cutting is not appropriate due to severe chip distortion. Therefore the analysis is applied to the material like AL6061-T6 and AL2024-T4 whose chip distortion is not so severe.

From the model prediction, it is shown that the fracture location, x_f, decreases as the inclination angle increases but it is not so sensitive to the variation of inclination angle. Two kinds of fractures are observed in oblique cutting: uniform fracture and inclined fracture according to the variation of fracture location. The uniform fracture can be predicted using the modified model. The inclined fracture occurs at every last corner of workpiece which a tool exits. The inclination of fracture is assumed as approximately same as the tool inclination angle. To predict the inclined fracture location, the equivalent initial tool distance, w_{eq}, is obtained and applied

to the modified model. In AL6061-T6 and AL2024-T4, the inclined fracture location is reasonably predicted. In the case of brittle material like AL390, more research must be continued due to different fracture mechanism. The uniform fracture could not be observed easily in this experiment because the workpiece is not wide enough. However most of burr formation in practice will be in steady state condition except last corner because the width of workpiece is much larger than undeformed chip thickness. The critical width of workpiece for the existence of uniform fracture is calculated.

References

1. Ko, S. and Dornfeld, D. A., "A Study on Burr Formation Mechanism", Trans. J. of Eng. for Materials and Technology, Vol. 113/1, pp. 75-87, Jan., 1991.
2. Ko, S. and Dornfeld, D. A.", Analysis and Modelling of Burr Formation and Breakout in Metal", Mechanics of Deburring and Surface Finishing Process, R. J. Stango & P. R. Fitzpatrick, eds., ASME, NewYork, 1989, pp79-91.
3. Usui, E., Hirota, A., and Masuko, M., "Analytical Prediction of Three Dimensional Cutting Process: Part 1. Basic Cutting Model and Energy Approach", Trans. of ASME, J. of Eng. for Industry, Vol. 100, pp. 222-228, May, 1978.
4. Rubenstein, C., "The Mechanics of Continuous Chip Formation in Oblique Cutting in the Absence of Chip Distortion. Part 1-Theory", Int. J. of Machine Tool Des. Res., Vol. 23/1, pp. 11-20, 1983.
5. Lau, W. S. and Rubenstein, C., "The Mechanics of Continuous Chip Formation in Oblique Cutting in the Absence of Chip Distortion. Part2-Comparison of Experimental Data with Deductions from Theory", Int. J. Mach. Tool Des. Res., Vol. 23/1, pp. 21-37, 1983.
6. Rubenstein, C., "A Simple Theory of Orthogonal Cutting", Int. J. Mach. Tool Des. Res., Vol. 4, pp. 123-156, 1965.
7. Datsco, J., in Material Properties and Manufacturing Process, John Wiley & Sons, New York, 1967.
8. ASM Metals Reference Book, Metals Park, Ohio, 1981.
9. Thomson, E. G., Yang, C. T. and Kobayashi, S., in Plastic Deformation in Metal Processing, The Macmilan Co., New York, 1965.
10. Lee, D. "The Effect of Cutting Speed on Chip Formation under Orthogonal Machining", Trans. ASME, J. of Eng. for Industry, pp. 55-63, Feb., 1985.